Coherent Population Trapping and Electromagnetically Induced Transparency

Carlos Sanchidrián

October 24, 2022

Contents

1 Introduction

The Coherent population trapping (CPT) and Electromagnetic Induced Transparency (EIT) are quantum phenomena based on quantum superposition of atomic states.

They arise from the fact that the atoms are optically pumped into a **dark non-absorbing state** by the excitation beams. Once pumped, atoms are trapped in that state because there is no way to spontaneously decay from there –hence the name-. A transparency window can be observed when a probe laser is scanned. In simple words "Imagine you can make a black wall transparent just by shining a certain light onto that wall. In principle, this is what happens to an atomic medium when it experiences electromagnetically induced transparency". In our case, the medium will be a cell of metallic vapor (Rb^{87}) but any alkaline atom can be used.

When one of the laser beams power is strongly enough to produce the dark state by itself the phenomenon is called Electromagnetic Induced Transparency (EIT).

To observe EIT or CPT, the minimum number of degrees of freedom is 3, that is, a 3 level-system, which usually implies 2 lasers or one plus a frequency modulator (EOM/OAM). In fact, the EIT can change to Electromagnetically Induced Absorption (EIA), a similar phenomenon where absorption is enhanced.

In this section, we will review the 2-level system, and the description of the 3-level system for a ladder and lambda configurations following the path of [1]. As both are equivalent, we will add Doppler effect in the section 2 in the ladder system, which will be studied experimentally. We will write the most general equations and then particularize for both cases.

CPT/EIT are two side of the same coin but are not the same and have different applications. The differences between them are explained in [2]

1.1 Energy Levels

CPT and EIT require atoms with specific energy levels.

For a three level system, (ground state=1,2, excited state=3) CPT requires two dipole allowed transitions (1-3) and (2-3) and one forbidden transition (1-2 is dipole forbidden, see Fig. (2)) .

It is typical to consider alkali atoms due to the good stability of the ground states in the s-shell. The frequency transitions of the hyperfine sublevels varies in the microwave range, and can be selected by a tunable laser.

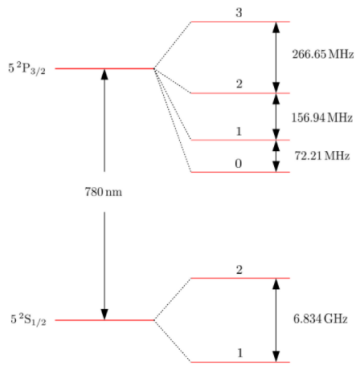

Figure 1: Energy levels of the D2 line at ^{87}Rb. The F value of each level is indicated.

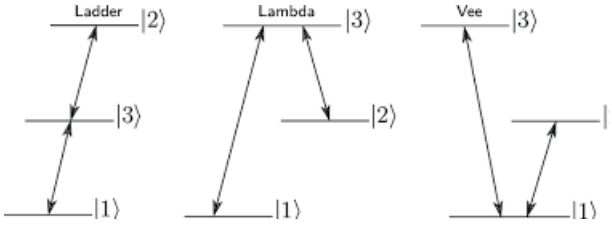

Figure 2: Different level configurations

Specifically, the natural abundance in Rb vapor is 72.17 % Rb85 and 27.83% Rb87. Rb85 is usually used for EIT because of it vapor pressure.

Nevertheless, we will focus on Rb87 because of its lower isospin.

There are several option for choosing the levels such as Lambda, Ladder or Vee type scheme as shown in figure 2 Ladder system configuration will be used in order to address the Rydberg states in the final setup. As it has been shown, counterpropagating beams can reduce the linewith of EIT due to a Doppler cancelation effect.

We will describe first a lambda system 3 in cold atoms and then we will study a ladder system in hot atoms, which require including Doppler effect.

We will focus on a few transitions. We will couple $5^2S_{1/2}F_2$ with $5^2P_{3/2}F_2$ for our (2-3) transition, and $5^2S_{1/2}F_1$ with $5^2P_{3/2}F_2$ for our (1-3) transition from a 780 nm laser, where F is the total angular momentum, F=I+J. As we intended, the (1-2) transition is dipole forbidden. The polarization of both beams are usually taken orthogonal in order to distinguish them.

The semi-classical Hamiltonian is given by the atomic harmonic oscillators (ground and excited states) and the interaction between the atom dipole $\vec{d}$ and the electric field $\vec{E}$.

$H = H_0 + H_I$ with

$$H_0 = \hbar \sum_e \omega_e |J, F, m_F\rangle\langle J, F, m_F| + \hbar \sum_g \omega_g |J', F', m'_F\rangle\langle J', F', m'_F|, \tag{1}$$

$$H_1 = -\vec{d}_{J'J} \cdot \vec{E} = -e\langle J', F', m'_F|\vec{r} \cdot \vec{\epsilon}|J, F, m_F\rangle \cdot E \cos(\vec{k}\vec{r} + \omega t + \varphi), \tag{2}$$

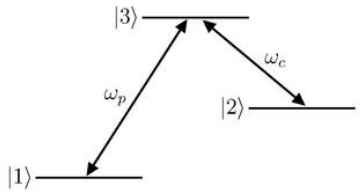

Figure 3: Energy levels at ^{87}Rb. A three-state Λ-type system

where e is the electron charge, $\vec{\epsilon}$ is the vector polarization. Rabi Frequency is usually defined as

$$\Omega_{J'J} = -\frac{\vec{d}_{J'J} \cdot \vec{E}}{\hbar}, \tag{3}$$

We generally choose the phase of the dipole matrix element to get a positive Rabi Frequency.

The dipole matrix element $\varrho = -e\langle J', F', m'_F|\vec{r}\cdot\vec{\epsilon}|J, F, m_F\rangle$ for each transition can be calculated with the python library Alkali Rydberg Calculator (ARC) using the commmand atom.getDipoleMatrixElement().

The laser's and dipole's phases can be dropped off from the formula and will be kept by the quantum state. This way is followed by some authors and shows the importance of the phases. Using $\varrho := |\vec{d}_{J'J}|$ and $\cos(\vec{k}\vec{r}+\omega t+\varphi) = \cos\phi$:

$$\Omega = \frac{\varrho \cdot E}{\hbar} \tag{4}$$

As we will see, the Rabi´s phases cancel when calculating the electric susceptibility so they are not relevant for physical purposes. The details can be found in [1]

The electric field amplitude is related with the power density of the source through the following formula:

$$I = \frac{2P}{\pi w^2} = \frac{\epsilon_o c E^2}{2}, \tag{5}$$

where w is the waist of the beam.

In order to not saturate the spectrum, the intensity must be under the saturation intensity (of the order of 1 W), defined as:

$$I_{sat} = \frac{h\nu}{(\sigma_e + \sigma_a)\tau} \tag{6}$$

where $h\nu$ is the photon energy at the signal wavelength, $\sigma_{e,a}$ are the emission and absorption cross sections at the emission wavelength and τ is the upper-state lifetime of the laser system.

1.2 3-Λ-system with cold atoms: EIT vs CPT

We start with a three-state Λ-type system and follow the approach of [1]. Without loosing generality, we define the states $|1\rangle = |5S_{1/2}, F = 1, m_F = 0\rangle$, $|2\rangle = |5S_{1/2}, F = 2, m_F = 0\rangle$ and $|3\rangle = |5P_{3/2}, F = 2, m_F = 1\rangle$ where $|1\rangle \leftrightarrow |3\rangle$ and $|2\rangle \leftrightarrow |3\rangle$ are dipole-allowed transitions stimulated by probe and coupling laser respectively and $|1\rangle \leftrightarrow |2\rangle$ is forbidden.

The total Hamiltonian is, as before, $H_T = H_0 + H_1$,

$$H_0 = \hbar\omega_1|1\rangle\langle 1| + \hbar\omega_2|2\rangle\langle 2| + \hbar\omega_3|3\rangle\langle 3| \tag{7}$$

$$H_1 = -\frac{\hbar}{2}\left[\left(\Omega_p(e^{i\phi_p} + e^{-i\phi_p})|1\rangle\langle 3| + \Omega_c(e^{i\phi_c} + e^{-i\phi_c})|2\rangle\langle 3|\right) + \text{H.c.}\right], \tag{8}$$

where $\phi_i = \vec{k}\vec{r} + \omega t + \varphi$, are the lasers´s phases and it has been used the cosine identity; $\cos x = \frac{1}{2}(e^{ix} + e^{-ix})$.

We can apply the RWA to H_1. The H_0 will not be modified because it is diagonal. After making the unitary transformation and neglecting the fast oscillating terms as before, the total Hamiltonian becomes

$$H_{T,I} = UH_TU^\dagger = -\frac{\hbar}{2}\begin{bmatrix} 2\omega_1 & 0 & \Omega_p e^{i\phi_p} \\ 0 & 2\omega_2 & \Omega_c e^{i\phi_c} \\ \Omega_p e^{-i\phi} & \Omega_c e^{-i\phi_c} & 2\omega_3 \end{bmatrix} \tag{9}$$

where Ω_p and Ω_c are the Rabi frequencies of the probe field and the coupling field respectively and $U = e^{-iH_0t} = \begin{bmatrix} e^{-i\omega_1 t} & 0 & 0 \\ 0 & e^{-i\omega_2 t} & 0 \\ 0 & 0 & e^{-i\omega_3 t} \end{bmatrix}$. We see that the Hamiltonian becomes time independent.

We can apply another rotation, $U = \begin{bmatrix} e^{-i\phi_p} & 0 & 0 \\ 0 & e^{-i\phi_c} & 0 \\ 0 & 0 & 1 \end{bmatrix}$, to get ride of the phases, but we will have to undo these transformations when calculating expected values. The Hamiltonian result simplified as:

$$H_{T,I} = -\frac{\hbar}{2}\begin{bmatrix} 0 & 0 & \Omega_p \\ 0 & -2(\Delta_1 - \Delta_2) & \Omega_c \\ \Omega_p & \Omega_c & -2\Delta_1 \end{bmatrix}, \tag{10}$$

where $2(\omega_1 + \omega_p)\mathbf{1}$ has been added to the Hamiltonian. The detunnings between the laser and the transition frequency are defined as $\Delta_1 = \omega_{31} - \omega_p$, $\Delta_2 = \omega_{32} - \omega_c$.

The Hamiltonian is diagonal in a new basis which is a rotation of the original basis in terms of the mixing angles θ, ϕ .

In the case that $\Delta_1 = \Delta_2 := \Delta$, the **dark state** and the **bright or dressed states** can be expressed as

$$\begin{aligned} |D\rangle &= \cos\theta|1\rangle - \sin\theta|2\rangle \\ |B^+\rangle &= \sin\theta\sin\phi|1\rangle + \cos\phi|3\rangle + \cos\theta\sin\phi|2\rangle \\ |B^-\rangle &= \sin\theta\cos\phi|1\rangle - \sin\phi|3\rangle + \cos\theta\cos\phi|2\rangle \end{aligned} \tag{11}$$

When the atoms are in the dark state, they will stay in this state indefinitely. It can not absorb or emit any photons from the applied fields. It is, therefore, effectively transparent to the probe laser, even when the laser is exactly resonant with the transition. Spontaneous emission from $|3\rangle$ can result in an atom being in this dark state or another coherent state, known as a bright state. Therefore, in a collection of atoms, over time, decay into the dark state will inevitably result in the system being "trapped" coherently in that state, a phenomenon known as coherent population trapping (CPT). This can be used to measure electric or magnetic field as shown in figure 4.

The relevant natural linewidth is therefore the linewidth of transition between the two lower levels, which as mentioned before is close to zero because the transition is electric-dipole forbidden. As the origin of the linewith is different from the EIT case, CPT is used in metrological applications such as frequency and B-field measurements. For CPT, the quantity of interest is the upper state occupation, which decrease dramatically in the dark state.

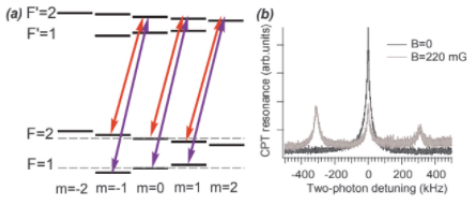

Figure 4: Transparency peaks due to Zeeman sublevels: When a magnetic field is applied, multiple transparency windows appears and the splitting between them is proportional to the magnetic field B

While the dark state remains at zero energy, the energy of the bare states is shifted by an amount:

$$E^{\pm} = \hbar\omega^{\pm} = \frac{\hbar}{2}(\Delta \pm \sqrt{\Delta^2 + \Omega_p^2 + \Omega_c^2}) \tag{12}$$

These eigenenergies can be found easily following the standard receipt: $|H - \lambda I| = 0$

$$|H - \lambda I| = -\frac{\hbar}{2}\begin{bmatrix} -\lambda & 0 & \Omega_p \\ 0 & -\lambda & \Omega_c \\ \Omega_p & \Omega_c & -2\Delta - \lambda \end{bmatrix}, (\lambda((\lambda - 2\Delta) + \Omega_c^2 + \Omega_p^2) = \lambda^2 - 2\Delta\lambda + \Omega_p^2 + \Omega_c^2 = 0 \tag{13}$$

In the resonance case ($\Delta = 0$) , the energy difference is proportional to the **Autler-Townes** frequency:

$\lambda = \Delta E = \frac{\hbar}{2}\Omega_{AT} = \frac{\hbar}{2}\sqrt{\Omega_p^2 + \Omega_c^2}$.

The difference in frequency of the absorbing peaks will be proportional to the field:

$$\Delta f = \Omega_{AT}/2\pi \rightarrow |E| = \frac{\hbar}{\varrho} 2\pi \Delta f \tag{14}$$

The mixing angles are:

$$\cos\theta = \frac{\Omega_c}{\sqrt{\Omega_p^2 + \Omega_c^2}}, \qquad \sin\theta = \frac{\Omega_p}{\sqrt{\Omega_p^2 + \Omega_c^2}}, \tag{15}$$

With $\tan 2\phi = \frac{\sqrt{\Omega_p^2+\Omega_c^2}}{\Delta}$.

To see the origin of EIT using the dressed-state picture above, consider the case of a weak probe.

The ground state becomes identical to the dark state from which excitation cannot occur.

Furthermore, when the probe is on resonance, we have usual dressed states relevant to EIT in the limit of a strong-coupling field and a weak probe.

$|B^+\rangle = \frac{1}{\sqrt{2}}(|2\rangle + |3\rangle)$

$|B^-\rangle = \frac{1}{\sqrt{2}}(|2\rangle - |3\rangle)$

2 Von Neumann equation

It can be shown that the most general equation for a decay process and is called the Gorini–Kossakowski–Sudarshan–Lindblad equation (GKSL equation), which can be written in a simple way as a function of the collapse operators V_i:

$$\dot{\rho}_{\mathrm{S}} = -\frac{i}{\hbar}[H, \rho_{\mathrm{S}}] + \mathcal{L}_{\mathrm{D}}(V_n, \rho_{\mathrm{S}})$$

$$\mathcal{L}_{\mathrm{D}}(V_n, \rho_{\mathrm{S}}) = \sum_n \left(V_n \rho_{\mathrm{S}} V_n^\dagger - \frac{1}{2}\left(\rho_{\mathrm{S}} V_n^\dagger V_n + V_n^\dagger V_n \rho_{\mathrm{S}}\right)\right)$$

A detailed derivation of this master equation is given in several works. It is also the most general (Markovian) way of mapping density matrix onto density matrices.

It is worthy to note that collapse operators V_n will be summed up within a unique operator in the case of being indistinguishable. Quantum systems are generally much more complicated than is feasible to include in our models. Such as complexities include interactions and collisions between atoms, and spontaneous emission and decays.

Each of these processes removes population (non-energy-conserving processes) or coherence (energy-conserving processes) from a given state, which is generally described by the density matrix ρ_S.

The Linblad (collapse) operators that take into account the decoherence and dephasing mechanisms are:

Decoherence (non-energy-conserving processes):

Natual decay rate: Arise from the inestability of the excited state. The decay is due to the interaction of the atom with the vaccum. To account for natural decay, we add in the phenomenological decay rate described by Γ using the atomic projector, $\sigma_{ij} = |i\rangle \langle j|$,

Transit time broadening: This effect arise from the motion of atoms in a finite time, called the transit time, during which the atom is present in the region where it can interact with the light field. If we express the typical velocity of the atoms as v and the size of the interaction volume as D, the interaction time is of the form D/v. If we consider that the gas of atoms is in thermodynamic equilibrium, each time that an atom leaves the interaction volume, it is replaced by an atom in the ground state.

Dephasing (energy-conserving processes):

Collisions: This effect arise from the motion of atom. The effect can be thought as a dephasing as well as they are inelastic.

Laser linewidth: The linewidth of the lasers induces a detuning in the atoms and consequently, a dephase in each level i.

To account for decoherence effects, we add in phenomenological dephasing terms described by γ using the atomic projector, $\sigma_{ii} = |i\rangle\langle i|$, the main effects are:

The residual Doppler shift is due to wavelength mismatch, which induce a dephase for each atom velocity class. There is not an analytical formula but is calculated integrating over the Boltzman distribution.

In the case of Rydberg states there is aditional sources of decoherence due to collisions a Rydberg blockade and blackbody decay.

The Von Neumann equation result in a master equation:

$$\dot{\rho}_{\mathrm{S}} = -\frac{i}{\hbar}[H, \rho_{\mathrm{S}}] + \frac{1}{2}\sum_{i,j,i\neq j}\Gamma_{i,j}(2\sigma_{ij}\rho_S\sigma_{ij}^{\dagger} - \rho_S\sigma_{ij}\sigma_{ij}^{\dagger} - \sigma_{ij}\sigma_{ij}^{\dagger}\rho_S) + \sum_i \gamma_i(2\sigma_{ii}\rho_S\sigma_{ii}^{\dagger} - \rho_S\sigma_{ii}\sigma_{ii}^{\dagger} - \sigma_{ii}\sigma_{ii}^{\dagger}\rho_S) \quad (16)$$

We assume here that the thermal occupancy of the relevant radiation field modes is completely negligible. For optical frequencies this approximation is easily justified.

We will now focus on the 3-lambda sytem described in. Using the collapse operators $V_1 = \sqrt{\Gamma_{31}}\,|1\rangle\langle 3|\,, V_2 = \sqrt{\Gamma_{32}}\,|2\rangle\langle 3|$, the master equation becomes:

$$\begin{aligned}\frac{d\rho}{dt} = \frac{-i}{\hbar}[H_{1,I}, \rho] + \frac{\Gamma_{31}}{2}(2\sigma_{13}\rho\sigma_{31} - \sigma_{33}\rho - \rho\sigma_{33} + \frac{\Gamma_{32}}{2}(2\sigma_{23}\rho\sigma_{32} - \sigma_{33}\rho - \rho\sigma_{33}) \\ + \frac{\gamma_{2depth}}{2}(2\sigma_{22}\rho\sigma_{22} - \sigma_{22}\rho - \rho\sigma_{22} + \frac{\gamma_{3depth}}{2}(2\sigma_{33}\rho\sigma_{33} - \sigma_{33}\rho - \rho\sigma_{33})\end{aligned} \quad (17)$$

We have assumed that $|2\rangle$ is a metastable state, so Γ_{21} will be dramatically smaller than Γ_{3j}. The Von Neumann equation rise to 6 out of 9 independent equations:

By the moment we set $\gamma_{2depth,3depth} = 0$ and γ_1 drops to zero, since conservation of energy prevents relaxations out of the ground state rising this equations:

$$\begin{aligned}\dot{\rho}_{11} &= \Gamma_{31}\rho_{33} + \frac{i}{2}(\Omega_p\rho_{13} - \Omega_p\rho_{31}) \\ \dot{\rho}_{22} &= \Gamma_{32}\rho_{22} + \frac{i}{2}(\Omega_c\rho_{23} - \Omega_c\rho_{32}) \\ \dot{\rho}_{33} &= -2\Gamma\rho_{33} + \frac{i}{2}(\Omega_p\rho_{13} - \Omega_p\rho_{31}) + \frac{i}{2}(\Omega_c\rho_{23} - \Omega_p\rho_{32}) \\ \dot{\rho}_{12} &= (i(\Delta_c - \Delta_p))\rho_{12} + \frac{i}{2}(\Omega_p\rho_{32} - \Omega_c\rho_{13}) \\ \dot{\rho}_{13} &= (\Gamma - i\Delta_p)\rho_{13} + \frac{i}{2}(-\Omega_c\rho_{12} + \Omega_p(\rho_{33} - \rho_{11})) \\ \dot{\rho}_{23} &= (-\Gamma - i\Delta_c)\rho_{23} + \frac{i}{2}(-\Omega_p\rho_{21} + \Omega_c(\rho_{33} - \rho_{22}))\end{aligned} \quad (18)$$

Where we have defined the total decay rate $\Gamma = (\Gamma_{31} + \Gamma_{32})/2$. These equations must be solved numerically in the case of CPT. However, this is not the case of EIT where all the population is mainly in $|1\rangle$.

2.1 EIT case

As mentioned, the atoms will primarily be in the ground state $|1\rangle$, with few atoms in the excited states. This allows us to write:

$$\rho_{11} \simeq 1,\ \rho_{22} \simeq 0,\ \rho_{33} \simeq 0 \quad (19)$$

And the three differential equations are:

$$\begin{aligned}\dot{\rho}_{12} &= (i(\Delta_c - \Delta_p))\rho_{12} + \frac{i}{2}(\Omega_p\rho_{32} - \Omega_c\rho_{13}) \\ \dot{\rho}_{13} &= (\Gamma - i\Delta_p)\rho_{13} + \frac{i}{2}(-\Omega_c\rho_{12} + \Omega_p(\rho_{33} - \rho_{11})) \\ \dot{\rho}_{23} &= (\Gamma - i\Delta_c)\rho_{23} + \frac{i}{2}(-\Omega_p\rho_{21} + \Omega_c(\rho_{33} - \rho_{22}))\end{aligned} \quad (20)$$

In the steady state, it simplifies as:

$$\frac{d\rho_{ij}}{dt} = 0 \rightarrow \dot{X} = MX + A \rightarrow X = -M^{-1}A \tag{21}$$

It turns out three equations that can be solved

$$\begin{aligned} \rho_{12} &= \frac{i(\Omega_p\rho_{32} - \Omega_c\rho_{13})}{2(i(\Delta_c - \Delta_p))} \\ \rho_{13} &= \frac{i(-\Omega_c\rho_{12} - \Omega_p)}{2(\Gamma - i\Delta_p)} \\ \rho_{23} &= -\frac{-i\Omega_p\rho_{21}}{2(\Gamma - i\Delta_c)} \end{aligned} \tag{22}$$

The weak probe assumption ($\Omega_p < \Omega_c$) allows us to drop any terms proportional to Ω_p^2, because Ω_p is proportional to our probe beam electric field magnitude. Looking at steady state solutions (where time derivatives vanish), we observe that ρ_{23} is first order in Ω_p. Thus, the term $i\Omega_p\rho_{32}$ is second order in Ω_p, and can be dropped under the approximation. We now have a nice coupled pair of equations:

$$\dot{\rho}_{21} = (i(\Delta_c\Delta_p))\rho_{12}i\frac{\Omega_c}{2}\rho_{13} \tag{23}$$

$$\dot{\rho}_{31} = (\Gamma - i\Delta_p)\rho_{13}i\frac{\Omega_p}{2}i\frac{\Omega_c}{2}\rho_{12} \tag{24}$$

Solving the equations we find:

$$\rho_{12} = \frac{\Omega_c\Omega_p}{4(i\Gamma + \Delta_c - \Delta_p)(i\Gamma + \Delta_p) + \Omega_c^2} \tag{25}$$

$$\rho_{13} = -\frac{2(\Gamma i(\Delta_c - \Delta_p))\Omega_p)}{4(\Gamma + i\Delta_p)(i\Gamma - \Delta_c + \Delta_p) - i\Omega_c^2} \tag{26}$$

2.2 From density matrix to susceptibility

The polarization of a medium is defined as the dipole moment per unit volume - if we let N be the number of atoms per unit volume, the polarization can be expressed in terms of the expectation of the dipole operator:

$$\mathbf{P} = N\langle\varrho\rangle = NTr(\rho\varrho) = N(\rho_{13}\varrho_{31} + \rho_{23}\varrho_{32} + \rho_{32}\varrho_{23} + \rho_{31}\varrho_{13}) \tag{27}$$

In (32), we computed the density matrix elements in the rotating basis, we must convert these elements in the regular basis by using the inverse transformations after (16), resulting in:

$$\mathbf{P} = N(\varrho_{13}\rho_{31}e^{i\omega_p t}e^{i\phi_p} + \varrho_{23}\rho_{32}e^{i\omega_c t}e^{i\phi_p} + H.c.) \tag{28}$$

We are looking for the linear susceptibility , given by the relation

$$\mathbf{P} = \epsilon_0\chi\mathbf{E} = \chi(\phi_p)\mathcal{E}_p\epsilon_0\frac{1}{2}e^{i\phi_p}(e^{i\omega_p t} + e^{-i\omega_p t}) + \chi(\phi_p)\mathcal{E}_c\epsilon_0\frac{1}{2}e^{i\phi_c}(e^{i\omega_c t} + e^{-i\omega_c t}) \tag{29}$$

From these last two equations, we can match the time dependent exponentials, giving us:

$$N\varrho_{13}\rho_{31}e^{i\phi_p} = \chi(\omega_p)\mathcal{E}_p\epsilon_0\frac{e^{i\phi_p}}{2} \rightarrow \chi = \frac{2N\varrho_{13}\rho_{31}}{\mathcal{E}_p\epsilon_0} \tag{30}$$

Adding the equation obtained before,

$$\chi = -\frac{2N\varrho_{13}\Omega_p}{\mathcal{E}_p\epsilon_0}\frac{2(\Gamma i(\Delta_c - \Delta_p))\Omega_p)}{4(\Gamma + i\Delta_p)(i\Gamma - \Delta_c + \Delta_p) - i\Omega_c^2} \tag{31}$$

We will now split χ into real and imaginary part

$$\mathrm{Re}(\chi) = -\frac{2N\varrho_{13}\Omega_p}{\mathcal{E}_p\epsilon_0}\frac{2(4(\Delta_c - \Delta_p)^2\Delta_p + (\Delta_c - \Delta_p)\Omega_c^2)}{16((\Delta_c - \Delta_p)^2(\Gamma^2 + \Delta_p^2) + 8((\Delta_c - \Delta_p)\Delta_p)\Omega_c^2 + \Omega_c^4} \tag{32}$$

$$\mathrm{Im}(\chi) = -\frac{2N\varrho_{13}\Omega_p}{\mathcal{E}_p\epsilon_0}\frac{8\Gamma(\Delta_c-\Delta_p)^2}{16((\Delta_c-\Delta_p)^2(\Gamma^2+\Delta_p^2)+8((\Delta_c-\Delta_p)\Delta_p)\Omega_c^2+\Omega_c^4} \tag{33}$$

We can see that for $\Omega_c = 0$, these equations reduce to a typical Lorentzian curve.

$$\mathrm{Re}(\chi) = -\frac{N\varrho_{13}\Omega_p}{\mathcal{E}_p\epsilon_0}\frac{\Delta_p}{(\Gamma^2+\Delta_p^2)} \tag{34}$$

$$\mathrm{Im}(\chi) = -\frac{N\varrho_{13}\Omega_p}{\mathcal{E}_p\epsilon_0}\frac{\Gamma}{(\Gamma^2+\Delta_p^2)} \tag{35}$$

2.3 3-ladder(Ξ)-system at room Temperature

We now study the case more relevant for the experiment, the ladder/cascade Ξ system. The states are defined now as in [4] $|1\rangle = |5S_{1/2}, F = 2\rangle$, $|2\rangle = |5P_{3/2}, F = 3\rangle$ and $|3\rangle = |5D_{5/2}, F = 4\rangle$ where $|1\rangle \leftrightarrow |2\rangle$ and $|2\rangle \leftrightarrow |3\rangle$ are dipole-allowed transitions stimulated by probe and coupling laser respectively and $|1\rangle \leftrightarrow |3\rangle$ is forbidden. H_0 is the same as (15) but the interacting part changes due to the relabel of states and H_1:

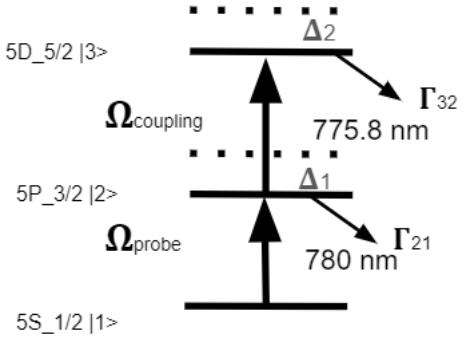

Figure 5: 3 level system with a ladder configuration following [7]

$$H_0 = \hbar\omega_1|1\rangle\langle 1| + \hbar\omega_2|2\rangle\langle 2| + \hbar\omega_3|3\rangle\langle 3| \tag{36}$$

$$H_1 = -\vec{d}\cdot\vec{E} = \frac{\hbar}{2}\left[(\Omega_p|1\rangle\langle 2| + \Omega_c|2\rangle\langle 3|) + \mathrm{H.c.}\right], \tag{37}$$

When Doppler effect is taken into account, the frequency observed by a moving atom is shifted by an amount $\omega v/c$. The detuning in his reference frame becomes:

$$\Delta_{i,D} = \Delta_i \pm k_i v, \text{ for i=[p,c]} \tag{38}$$

The total Hamiltonian turns out to be

$$H_{T,I} = \frac{\hbar}{2}\begin{bmatrix} -2\Delta_1 & \Omega_p & 0 \\ \Omega_p & -2\Delta_2 & \Omega_c \\ 0 & \Omega_c & -2\Delta_3 \end{bmatrix} = \frac{\hbar}{2}\begin{bmatrix} 0 & \Omega_p & 0 \\ \Omega_p & -2\Delta_{p,D} & \Omega_c \\ 0 & \Omega_c & -2(\Delta_{p,D}+\Delta_{c,D}) \end{bmatrix} \tag{39}$$

Where $\Delta_1 = 0,\ \Delta_2 = \Delta_1 + \Delta_{p,D},\ \Delta_3 = \Delta_2 + \Delta_{c,D}$.

From the linear dispersion K(ω), the absorption coefficient ($\alpha = 2\pi\chi/\lambda$) and the refractive index of the atomic vapor of the probe beam are obtained averaging over the Maxwell distribution as:

$$\alpha = \frac{2N\omega_p d_{eg}}{\mathcal{E}_p c\epsilon_0}\int P(v)\mathrm{Im}(\rho_{12})dv \tag{40}$$

$$n-1=\frac{Nd_{eg}}{\mathcal{E}_p\epsilon_0}\int P(v)\mathrm{Re}(\rho_{12})dv \tag{41}$$

The transmission is related with the absorption coeffcient as:

$$T=\exp(-\alpha L) \tag{42}$$

The Lindblad equation can be resolved analytically in the steady state in analogous way to the Λ system. The equation in the EIT limit of ρ_{12} turns out to be

$$\rho_{12}=\frac{i\Gamma_{13}\Omega_p}{\Gamma_{12}\Gamma_{13}+\Omega_c^2} \tag{43}$$

where $\Gamma_{12}=-i\gamma_{21}-i\Delta_p-i\omega_p v/c$, $\Gamma_{13}=-i\gamma_{31}-i(\Delta_p+\Delta_c)-i(\omega_p-\omega_c)v/c$ and $\gamma_{ij}=\frac{\Gamma_i+\Gamma_j}{2}$.

This equation was solved analytically (see [7]) making approximations and it was thought that the Doppler effect would spoilt the EIT linewidth. Nevertheless, the the integration in 40 can be carried out analytically by using the residue theorem. When the Maxwell's velocity distribution is replaced by the modified Lorentzian velocity distribution with FWHM=$2W_D$ ($f(kv)=\frac{W_D}{\pi(W_D^2+(kv)^2)}$), the poles become $kv=iW_D$. Such a technique has been widely employed by many authors, in resonance, eq 40 turns out to be [11].

$$K(\omega)=\frac{\omega}{c}+\frac{2N\omega d_{eg}}{\mathcal{E}_p c\epsilon_0}\frac{\sqrt{\pi}(\omega+i\gamma_{31})}{|\Omega^2|-(\omega+i\gamma_{21}+i\Delta\omega_D)(\omega+i\gamma_{31})} \tag{44}$$

It is remarkable the simple form in which the Doppler linewidth ($\Delta\omega_D=\sqrt{\frac{8kT\ln 2}{mc^2}}\omega_0\simeq$500 MHz at room temperature) is added to the formula of EIT. As we will see, thanks to Doppler effect, the linewidth of EIT is reduced.

Next, The Linblad equation is solved in the steady state with python:

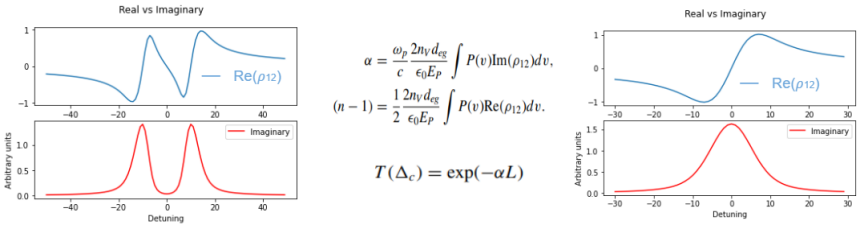

Figure 6: Real vs Imaginary part of ρ_{12} for a 3 level system. EIT is observed when the coupling laser is on

The intensity of EIT as well as the linewidth depends mostly on the coupling's Rabi frequency as shown in figure 7.

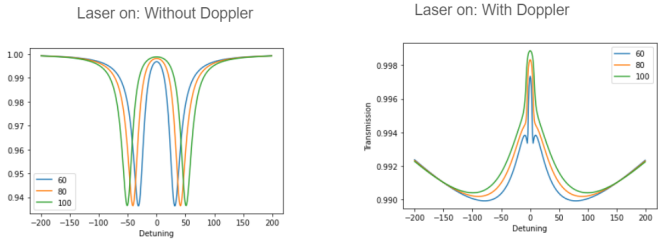

Figure 7: EIT for 3-level system varying Ω_c: Dark states (absorption peaks) are splitted directly proportional to $\hbar\Omega$ according to (21). Doppler effect introduced a curved background as expected. The horn peaks in the Doppler case are due to numerical error and will not be observed.

The resason of the the reduction of the linewidth, as well as the curved background, is on the effect that the Doppler shift induce on each velocity class as shown in figure 8:

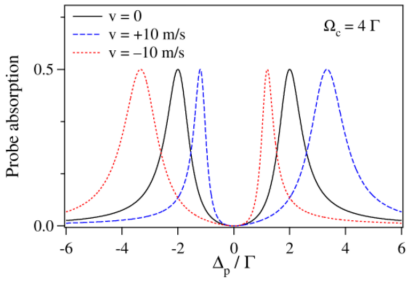

Figure 8: The solid curve is for stationary atoms, while the dashed (dotted) curve is for atoms moving with v=+10(10) m/s. The Autler-Townes doublet for the moving atoms is shifted to the right or left so that they fill in the transparency region for stationary atoms.

In 9 we see the dependence of the absorption coefficient of the transparency peaks with power. Surprisingly, the second peak in the off-resonant case increase with power. The opposite happens with the probe laser A compromise between the linewidth and the transmission must be achieved experimentally. We now compare

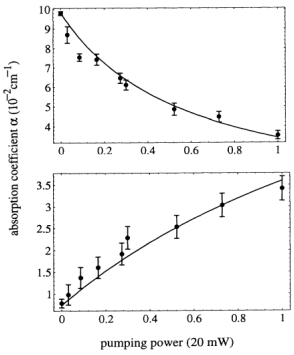

FIG. 7. Absorption coefficient versus pumping power for (a) $\Delta_2=\Delta_1=0$ and (b) $\Delta_2=-550$ MHz and $\Delta_1\simeq 550$ MHz (the two-photon absorption peak is slightly shifted from $\Delta_1=-\Delta_2$). Solid line, theoretical prediction [the parameters are the same as in Figs. 5 and 6, with the abscissa equal to Ω_1^2 in units of (92 MHz)^2].

Figure 9: Absorption coefficient vs pumping power.

our simulation with the experimental and theoretical result of [7]. They arrive to an analytical formula in the EIT limit. When the coupling laser is on, a transparency window appears at the center, when coupling laser is off, the typical Lorentzian curve is recovered 10.

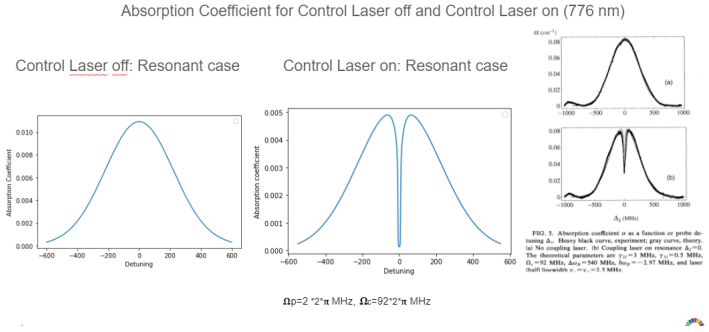

Figure 10: Absorption coefficient comparison between numerical simulation and experimental results from [7]. The linewidth is reduced with increasing temperature due to Doppler effect cancellation when counter-aligning both lasers.

It can be noticed that the line-width of the EIT (1-10MHz) window can be narrower than the natural linewidth of EIT $\gamma \simeq 6 * 2\pi$ MHz . That is, due to **Doppler effect** subnatural linewidth (lower than the natural decay rate) can be achieved as experimentally shown in [8]. This effect is expressed through the following simple

formula, that is derived in [9] comparing with the FWHM of the Lorentzian function:

$$\Gamma_{EIT} = \frac{\Omega_c^2 + \Omega_p^2}{W} \tag{45}$$

Which in the limit of no doppler effect is equivalent to the famous homogeneously broaden system due to the decaying rate γ:

$$\Gamma_{EIT} = \frac{\Omega_c^2 + \Omega_p^2}{\gamma} \tag{46}$$

The variety of linewidth formulas is due to different regimes and must be taken carefully. I. e., for the limit of low probe field ($\Omega_p < \Omega_c(\gamma/W)$), the EIT linewidth takes the following form [10]:

$$\Gamma_{EIT} = \frac{\Omega_c \Omega_p}{\gamma} \tag{47}$$

3 Application for measuring Electromagnetic Field

We have seen that the control laser **dresses** the atom in a new basis. The energy difference is proportional to the Rabi frequency in the resonance case.

Similarly, the result of an AC field on the atom is thus to shift the strongly coupled **bare atom energy eigenstates** into two states $|+\rangle$ and $|-\rangle$ which are now separated by $\hbar\Omega$ (Autler Townes Regime).

This picture has been used to measure E-fields that couples the lower excited states with Rydberg states. These states have a large dipole moment, which makes them really suitable for detect low signals.

The standard scheme for measuring E-fields with vapor atoms consist on a four level system in which two lasers are necessary, one for the probe, and another for the control.

Due to economic constraints, we looked for a cheaper applications of EIT with only one laser. EIT has been previously demonstrated with only one laser using an Electro Optical Modulator to generate two sources out of one, but we cannot address the Rydberg states with a diode laser. In fact we can only address the level $5P_{3/2}$ with one laser, therefore, the only levels accessible ($5P_{1/2}$ (magnetic transition), $5D_{5/2}$, $6S_{1/2}$,...) have a lower dipole moment and make them not suitable for communications, besides, they lay in the (1-100) THz range, which are difficult to detect at the moment.

We will now review the possibility of building a Quantum Radio Frequency sensor based on 3 diode laser. There have been experimental setups in a cascade level system to address the Rydberg states.

In general, for a n-level system in EIT regime, there will be n-2 transparency windows and n-1 transparency peaks, but this depends on the level scanned and the parameters chosen.

This is the case of [4], where they use a 5 level system to detect E-field. Their work is explained in another document.

References

[1] Thesis: Electromagnetically induced transparency, Erickson Wes

[2] Eur. Phys. J. D (2017) 71: 38, Coherent population trapping (CPT) versus electromagnetically induced transparency (EIT), Sumanta Khan, Molahalli Panidhara Kumar, Vineet Bharti and Vasant Natarajan

[3] REVIEWS OF MODERN PHYSICS, VOLUME 77, APRIL 2005, Electromagnetically induced transparency: Optics in coherent media

[4] PHYSICAL REVIEW A 100, 063427 (2019): Electromagnetically induced transparency, absorption, and microwave-field sensing in a Rb vapor cell with a three-color all-infrared laser system

[5] Optics Communications 190(1-6):221-229: Electromagnetically induced transparency in N-level cascade schemes

[6] OPTICS LETTERS / Vol. 37, No. 18 / September 15, 2012: Three-photon electromagnetically induced transparency using Rydberg states

[7] PHYSICAL REVIEW A VOLUME 51, NUMBER 1 JANUARY 1995: Electromagnetically induced transparency in ladder-type inhomogeneously broadened media: Theory and experiment

[8] Subnatural linewidth using electromagnetically induced transparency in Doppler-broadened vapor

[9] September 1, 2006 / Vol. 31, No. 17 / OPTICS LETTERS: Decoherence of electromagnetically induced transparency in atomic vapor

[10] Narrowing of EIT resonance in a Doppler Broadened Medium

[11] J. Opt. Soc. Am. B / Vol. 31, No. 4 / April 2014, Crossover from electromagnetically induced transparency to Autler–Townes splitting in open ladder systems with Doppler broadening, Chaohua Tan and Guoxiang Huang